Enhancement of Photocatalytic And Biological Activities of Chitosan/Activated Carbon Incorporated With TiO_2 Nanoparticles

Medhat E. Owda
Al-Azhar University
Ahmed S. Elfeky
Al-Azhar University
Ragab E. Abouzeid (r_abouzeid2002@yahoo.com)
National Research Centre https://orcid.org/0000-0002-1501-3336
Ahmed K. Saleh
National Research Centre
Mohamed A. Awad
Al-Azhar University
Hitham A. Abdellatif
Al-Azhar University
Fakher M. Ahmed
October 6 University
Ahmed S. Elzaref
Al-Azhar University

Research Article

Keywords: Chitosan, Activated charcoal, Photodegradation

Posted Date: May 24th, 2021

DOI: https://doi.org/10.21203/rs.3.rs-473585/v1

Version of Record: A version of this preprint was published at Environmental Science and Pollution Research on October 23rd, 2021. See the published version at https://doi.org/10.1007/s11356-021-17019-y.

Abstract

A Novel and sustainable chitosan (CS)/ activated charcoal (AC) composites were prepared by cross linking with epichlorohydrine (ECH) to form a porous structure. Different titanium dioxide nanoparticles (TiO_2 NPs) concentrations (0, 0.2, 0.4, and 0.8% w/w) were added to enhance the photocatalytic, antibacterial, larvicidal, and pupicidal activities efficiency toward rose bengal (RB) dye and the Culex Pipiens. The composites were characterized by FT-IR, XRD and SEM. The SEM images revealed the porous structure of CS/AC and TiO_2 nanoparticles were uniformly distributed in the CS/AC matrix. The degradation of RB dye was used to test the photocatalytic behavior of the composites. Supporting TiO_2 on a CS/AC matrix resulted in a significant increase in photocatalytic performance. The antibacterial activities supported by CS/AC/TiO_2 NPs were evaluated by bacterial growth inhibition against *B. subtilis*, *S. aureus, E. coli and P. aeruginosa*. The results showed that CS/AC/TiO2 NPs composite has an inhibitory effect and therefore considered as antibacterial agents. CS/AC/0.4%TiO_2NPs showed maximum efficacy against larvicidal activity and pupicidal of mosquito vector which recorded 99.00 ± 1.14, 95.00 ± 1.43, 92.20 ± 2.64 for first, second and third larval instars and 66.00 ± 2.39 for pupal mortality, while the repellent activity reported high protection at 82.95 ± 2.99 with 3.24 mg/cm^2 dose compared to control DEET.

Introduction

Chitosan (CS) is a linear heteropolysaccharide consisting of n-acetylglucosamine and 1,4-β- glucosamine, which derived from the deacetylation of chitin (Aragunde et al. 2018). It is insoluble in water as a results of the bonds between the polymer chains with hydrophilic nature, nontoxicity, and biodegradability (Cheung et al. 2015). Moreover, it is structure contains many free and active groups of ($-NH_2$) and (−OH), that can form coordination bonds with the empty orbital of metal elements (Xiong et al. 2013; Zhao et al. 2013; Luo et al. 2015). Therefore, CS biopolymer has been widely used to remove dyes and metal ions and become increasingly important in environmental biotechnology. In particular, CS as adsorbents has the advantages of being low cost, renewable, abundant, ecofriendly, multifunctional and, non-toxic and causing no secondary pollution. However, the use of CS as an adsorbent in wastewater treatment technologies is still limited due to its high solubility in an acidic medium, filtration ability, poor mechanical properties, and swelling of the aqueous medium. However, due to its high solubility in an acidic medium, filtration efficiency, poor mechanical properties, and swelling of the aqueous medium, the use of CS as an adsorbent in wastewater treatment technologies is still limited. A very effective way to overcome these limitations and enhance the physiochemical properties of the CS biopolymer is chemical modification by cross linking reaction using epichlorohydrin (ECH) with activated charcoal (AC) in the presence of metal oxides such as TiO_2. AC is also commonly used in water treatment, although it has some of technological drawbacks, including a high cost and difficulty in recovering it (Jung et al. 2016a, b; Hassan et al. 2017). AC particles have been encapsulated in a polymeric support, predominantly CS, to overcome these drawbacks. The use of this biological macromolecule produces composites with lower costs, better mechanical properties, and a higher number of functional groups (Afzal et al. 2018). TiO_2 is

an inert, nontoxic, chemically stable, biocompatible, and cheap material having been approved as safe for use in food and materials in contact with food by Food and Drug Administration (FDA) TiO2 is a nontoxic, chemically stable, biocompatible, and inexpensive substance that has been licenced by the Food and Drug Administration for the safe use in food and products that come into contact with food (FDA) (Zhou et al. 2009; Othman et al. 2014; El-Wakil et al. 2015; Zhang et al. 2017). The photocatalytic activity of TiO_2 nanoparticles is higher than that of bulk TiO_2 particles due to its high surface area to volume ratio. When exposed to ultra violet (UV) light, TiO_2 nanoparticles have a higher band gap energy and generates electron hole pairs on its surface, which improves their efficiency Due to their high surface area to volume ratio, TiO_2 nanoparticles have a higher photocatalytic activity than bulk TiO_2 particles. TiO_2 nanoparticles have a higher band gap energy and produce electron hole pairs on their surface when exposed to UV light, which improves their performance. (Maneerat et al. 2003; Onda et al. 2005; Lian et al. 2016). However, the tendency of nanosized TiO_2 to agglomerate reduces its performance (Qian et al. 2011; Lin et al. 2015). This random agglomeration of TiO_2 nanoparticles reduces the surface area of the particles and lowering their photocatalytic activity (Li et al. 2010; Lin et al. 2015). Photodegradation of organic pollutants, gas sensor, lithium battery processing, white pigments, wound healing, and drug delivery systems have been described as applications for TiO_2 NPs (Ali et al. 2015; Zhang et al. 2017). The addition of TiO_2NPs to food packaging films has been shown to enhance the films' physical, thermal, and mechanical properties(Xing et al. 2012). Over the resent few years, some studies have been reported the fabrication of CS with other composites to enhance the antimicrobial activity against pathogenic microbes such as CS/AgCl–TiO_2 (Moqeet Hai et al. 2019; Elfeky et al. 2020), hydroxyapatite/CS/TiO_2 (Li et al. 2019a) CS/silk fibroin/$Mg(OH)_2$(Eivazzadeh-Keihan et al. 2021) and CS/curcumin(Zhang et al. 2021). Mosquitoes are responsible for transportation of many pathogenic agents to human worldwide (Benelli et al. 2018). *C. pipiens L*. (Diptera: Cuicidae) recorded as one of the most widely dispensed mosquitoes in the world. It is called house mosquito and widely distributed in the urban areas and lives near people (Bernard et al. 2001; Oz et al. 2013). From this important, the research today diverted to find alternative agents that possess bioactive chemicals which act as insecticides, repellents as well as growth inhibitors (Murugan et al. 1996). The aim of this study was to produce crosslinked CS/AC/ by ECH and then incorporated with different concentrations of TiO_2 NPs as a suitable candidate for the removal of anionic dyes, such as rose bengal (RB) dye, assess its photodegradation properties and to evaluate the biological activities of the composites.

Experimental

Materials

Chitosan [80%–95% deacetylated, average molecular weight (MW) 9.0 × 106 Da], Titanium dioxide (TiO_2) nanoparticles Activated charcoal and Epichlorohydrin were purchased from Sigma-Aldrich. All the other chemicals were analytical reagent grades and used without further purification.

Methods

Preparation of the Composite CS/AC/ TiO_2NPs

Chitosan solution (1% w/v) was prepared by dissolving 1 gm of CS powder in 100 ml of a 1% (w/w) aqueous solution of acetic acid and stirred on magnetic stirrer for at least 3 hs at room temperature (until the solution became homogenous). Then half gram of AC was added to the CS solution until reaching a more uniform dispersion by ultrasound for 20 min then, 1 ml of ECH aqueous solution was added and stirred vigorously for cross-linked reaction for another 1 h. Different concentrations of TiO_2NPs were added to the solution and stirring for 30 min. The final product was obtained by immersed in a coagulation bath (50 ml of sodium hydroxide solution (5 mmol L^{-1})) for 2 hrs. , then the samples were separated from solution by centrifugation at 10000 rpm for 10 min and washed with deionized water. The obtained composite was dried at 100 °C, then ground in mortar to homogenous fine powder and used for photodegradation and biological studies.

Characterization

The morphology structure was carried out by scanning electron microscopy (SEM, Quanta-250 conducted with EDAX). Fourier transforms infrared spectroscopy (FT-IR) was performed by the KBr method on a Mattson 5000 spectrometer (Unicam, UK). The X-ray diffraction (XRD) was identified using X-ray diffractometer (PANa-lytical, Netherlands) at 25°C with Cu Kα a monochromatic radiation source (λ=0.154 nm, 2θ = 5°: 80°, and scanning time 5 min).

Application of prepared composites

Photodegradation procedure

The photocatalytic activity of CS/AC and CS/AC/TiO_2 are assessed utilizing the photocatalytic degradation of RB as reaction probe in beaker with stirring. For photocatalytic experiments, 100 ml (7.9 ppm) solution RB (C20H2Cl4I4Na2O5, M.Wt. 1017.65, LABA Chemie, CI # 45440), Scheme 1, was taken into the reactor with the required amount of the catalyst. Prior to irradiation, the solution was attractively blended in obscurity for 10 min to accomplish the adsorption equilibration of the framework. After irradiations utilizing UV- lamp (20 W), testing samples were removed at various time intervals, filtered and afterward poured in quartz cell. The RB concentration was determined by utilizing Lambda UV/vis spectrophotometer (Perkin Elmer) at λ = 540 nm at different times. All photocatalytic reactions were performed at room temperature.

The photodegradation efficiency was calculated by the following equation:

$$\text{Photodegradation efficiency } (\%) = \frac{C0 - Ce}{C0} \times 100$$

Where C_0 is the initial concentration of dye and Ce is the final concentration of dye after illumination by UV- light.

Biological activities

Antibacterial activity

Antibacterial activity of the prepared composites (CS/AC) at three different concentrations of TiO_2 NPs (0.2, 0.4 and 0.8) were investigated quantitatively by using broth (turbidity) inhibition method depending on the optical density (OD), against Gram negative *Escherichia coli* ATCC 8739(*E. coli*)and *Pseudomonas aeruginosa* ATCC 9027(*P. aeruginosa*) and Gram positive *Bacillus subtilis* ATCC6633 (*B. subtilis*) *Staphylococcus aureus* ATCC25923 (*S. aureus*), as reference strains for antibacterial assay, and obtained from the American Type Culture Collection (ATCC). Broth inhibition approach was conducted in flask (50 ml) containing 10 ml of Luria–Bertani (LB) broth media which composed of (g/l): peptone 10, yeast extract 5 and NaCl 5. To prepare the preinoclume, the strains were grown in LB broth at 30 °C and 200 rpm for 24 h. After cultivation time, each flask containing 10 ml of LB media was inoculated (100 µL) with the model bacteria used (OD at 660 nm reached 0.3) and assessed for antibacterial by adding 100 mg of the prepared composites, then incubated in shaking incubator 200 rpm at 30 °C for 24 h. The control was performed by growing the model bacteria at the same conditions without adding the composites. After time consumed, the bacterial growth was measured by taking the OD at 600 nm and the results will be expressed as growth inhibition % by the formula (Adel et al. 2019): Growth inhibition % = $(OD_{control} - OD_{sample})/ OD_{control}$ X100

Autoclaved all the required materials used in this experiment. Triplicate experiments were carried out for each composite.

Larvicidal and pupicidal activity:

The larvicidal and pupicidal activity of synthesized CS/AC/TiO_2 (0.2, 0.4and 0.8%) against the *C. pipiens* was evaluated by using the standard method bioassays(Williams et al. 1986). Each concentration was made separately at five different test concentrations (2, 4, 6, 8 and 10 ppm) of aqueous CS/AC/TiO_2 (0.2, 0.4, and 0.8%). To evaluate the larvicidal and pupicidal activity of synthesized CS/AC/TiO_2 (0.2, 0.4 and 0.8%), 25 larvae and pupae of *Cx. Pipiens* were separately and exposed to 100 ml of test concentrations. Also, the control (without CS/AC/TiO_2) was run to test the normal mortality. After that time, the mortality, which was particular after different hours of treatment, at the time of the experiment. No food was given to the larvae during the experiment. The experiments were repeated five times to confirm the results. The performance data was subjected to probate analysis. Mortality was corrected with Abbott's formula.

Repellency activity*:*

Standard cages (30x30x30 cm) were applied to test the repellent activity of the selected material. Different concentrations from the CS/AC/TiO_2 were directly applied onto 5x6 cm of abdomen surface of pigeon after feathers removal from the abdomen to correct the repellency with *C. pipiens* compared with commercial repellent DEET (N. N. diethyl-meta-roulamide) (Johnson Wax Egypt) as a positive control. After 10 minutes, the treated pigeons were placed in the cages containing 50 *C. pipiens* starved females

for three hours. Each test was repeated three times to get a mean value of repellent activity (Shehata 2019). After treatments, the number of unfed females were counted and calculated according: Repellency % = (%A - %B / 100 - % B) x 100 where:

A = percent of unfed females in treatment.

B = percent of unfed females in control.

Table 1: Larval and pupal toxicity of CS/AC/TiO_2 (0.2%) against the filariasis vector *Cx. Pipiens*

Targeted Instars	Mortality (%)				
	2 ppm	4ppm	6 ppm	8 ppm	10 ppm
I	27.00 ± 2.54	33.10 ± 3.78	41.10 ± 2.58	49.30 ± 1.14	59.20 ± 1.22
II	24.60 ± 2.30	27.20 ± 1.48	34.60 ± 1.81	41.20 ± 2.58	47.00 ± 1.73
III	23.80 ± 2.38	26.40 ± 2.50	31.20 ± 3.42	37.20 ± 3.11	42.20 ± 2.58
IV	21.40 ± 2.60	23.80 ± 1.64	28.00 ± 2.64	31.40 ± 2.96	38.00 ± 3.16
Pupa	18.60 ± 2.07	25.40 ± 2.30	27.80 ± 1.78	30.20 ± 2.58	33.00 ± 2.91
Mortality rates are means ± SD of five replicates. No mortality was observed in the control.					

Table 2: Larval and pupal toxicity of CS/AC/TiO_2 (0.4%) against the filariasis vector *Cx. Pipien*

Targeted Instars	Mortality (%)				
	2 ppm	4 ppm	6 ppm	8 ppm	10 ppm
I	40.00 ± 2.14	61.60 ± 3.72	73.20 ± 1.98	94.40 ± 1.17	99.00 ± 1.14
II	36.60 ± 2.45	57.20 ± 1.98	67.60 ± 1.71	86.20 ± 2.38	95.00 ± 1.43
III	30.80 ± 2.38	42.40 ± 2.50	61.20 ± 3.42	72.20 ± 3.14	92.20 ± 2.64
IV	22.40 ± 2.60	36.80 ± 1.64	51.00 ± 2.64	63.40 ± 2.56	81.00 ± 3.19
Pupa	18.60 ± 2.07	28.40 ± 2.30	43.80 ± 1.78	54.20 ± 2.18	66.00 ± 2.39

Table 3: Larval and pupal toxicity of CS/AC/TiO_2 (0.8%) against the filariasis vector *Cx. Pipiens*

Targeted Instars	Mortality (%)				
	2 ppm	4ppm	6 ppm	8 ppm	10 ppm
I	32.10 ± 1.92	47.40 ± 2.30	58.00 ± 1.70	71.00 ± 1.58	93.00 ± 3.16
II	28.40 ± 2.74	41.80 ± 1.30	53.80 ± 2.28	66.00 ± 2.12	81.00 ± 2.44
III	22.00 ± 2.01	31.60 ± 3.04	42.60 ± 2.64	56.20 ± 1.54	72.90 ± 2.23
IV	19.20 ± 2.16	23.80 ± 1.92	37.40 ± 2.30	44.20 ± 3.11	65.00 ± 2.14
Pupa	12.90 ± 2.38	18.20 ± 2.70	25.20 ± 3.39	39.40 ± 2.96	53.00 ± 2.91

Results And Discussion

SEM Analysis

Figure 1a shows that the surface morphology of CS, CS/AC and CS/AC/TiO_2, the surface structure of CS smooth and nonporous while the SEM Image of CS/AC crosslinked with ECH was a rough and heterogonous surface with evident cavities and irregular pore size figure 1b. In figure 1c the TiO_2 NPs was distributed uniformly in the matrix as evidenced by images of the composites, with some agglomeration and porous structure which providing the surface area that can be play essential role in the photodegradation of RB dye

FT-IR Analysis

The functional groups of CS/AC and CS/AC/TiO_2 spectrum were determined using FT-IR analysis which revealed the following characteristic peaks in figure 2: The bands from 3300-3450cm^{-1}(stretching vibrations of –OH and $–NH_2$ bonds), which may be due to electrostatic interaction with N-H-O-Ti. The band at 2870 cm^{-1} (stretching vibrations of CH_2), 1650 cm^{-1} (C-O stretching of primary amide), 1561 cm^{-1} (N-H bending of secondary amide group), 1421cm^{-1} in CS-AC due to C-N axial deformation (amine group); C-O stretching, 1380 cm^{-1} (C-N stretching vibration). The band at 1150 cm^{-1}(C-O-C glycosidic bonds, Ti-O-C bending mode, Ti-OH) bond in both (CS-AC-TiO_2 (0.2%,0.8%)and broadening at 1090 cm^{-1} (skeletal vibration of C–O)(Jawad and Nawi 2012; Danalıoğlu et al. 2017). The band at 450cm^{-1} is due to the bending vibration of Ti–O–Ti bonds(Bineesh et al. 2010).These peaks confirmed that the AC was successfully grafted with the chains of CS-ECH with $TiO_2$by the chemical interactions, such as hydrogen bonding formation between oxygen groups of AC and functional groups of the CS (Sharififard et al. 2018). The presence of amide, amine, and hydroxyl functional groups together with TiO_2 metal oxide confirms that it well-mixed and supports to effective dye removal through the RB dye photodegradation process.

XRD analysis

XRD patterns of CS/AC, CS/AC/TiO_2 shown in figure 3. As we can see from the XRD of CS/AC, two peaks are appearing at about 25° and 42° corresponding to reflection in the (002) plane and the (100) plane of aromatic layers in carbon with broad characteristic peak of chitosan at around 16°. The patterns of CS/AC with different percent of TiO_2 revealed the presence of TiO_2 nanoparticles with the peaks at 25.2°, 37.9°, 44.7°, 47.3°, 54.3° and 64°, which can be indexed as (101), (004), (200), (105), (211), and (204) planes of an anatase TiO_2.

Application of prepared composites

Photodegradation activity

Effect of AC/CS, TiO_2 and AC/CS/TiO_2components on RB degradation.

Firstly, the three components will be examined individual and then together to determine the viability to enhance the catalytic performance.0.1 g photocatalysts were added into 100 of RB solutions and 7.9 ppm dye concentration. As shown in Figure 4, the photodegradation percentage are 73.1, 75.3 and 91.9 % for samples CS/AC, TiO_2 and CS/AC/TiO_2 NPs, respectively. The composite demonstrated higher photocatalytic activity than of the CS/AC and TiO_2 under UV light irradiation. This occurrence believed to be related to the higher degree of interphase contact that can be achieved at the TiO_2 surface with activated carbon and chitosan (Dai et al. 2013).

Effect of different nanoTiO_2 contents on AC/CS

It is well known that, TiO_2 is the most efficient candidate for photocatalysis reactions and the addition at low concentration to CS/AC has led to increase the photodegradation efficiency. The photocatalytic performances at different TiO_2 NPs contents (0.2, 0.4 and 0.8 %) were assessed by degrading RB dye under UV illumination. The adsorption of dye has been conducted in dark and the data reveals that only 10 - 20% was adsorbed for all prepared TiO_2 percentage on CS/AC photocatalysts. Figure 5 (a, b) shows the photodegradation efficiency with different contents of TiO_2 NPs and relation between RB concentration and illumination time within 120 min.

The results shown that, the rate of photodegradation of RB was firstly increased with increasing the amount of TiO_2 NPs but finally, it decreased after a certain amount. This can be attributed to the fact that as the amount of dopant increases, the exposed surface area also increases, but after a certain limit i.e. 0.4%, if the concentration of TiO2 TiO_2 NPs is increased further, there were no increase in the exposed surface area of the photocatalyst. This can be thought of as a saturation point; moreover, any increase in the number of dopant contents had little or no effect on the photolysis rate of the RB dye, since any increase in the TiO_2 NPs percentage beyond this saturation point would only increase the thickness of the catalyst layer. This was confirmed by performing a reaction with a different ratio of denatured TiO_2 NPs from 0.2% to 0.8%. The limit of saturation point appeared at 0.4% of TiO_2 NPs after that increasing the amount led to decreased the dye degradation (Sharma et al. 2013) as seen in Figure 5 (a,b)

Effect of concentration of RB dye

The effect of RB dye concentration keeping the catalyst loading concentration constant at 100 ml of dye solution, and the experiment is performed by adding 0.1 g/l of catalysts to different initial RB concentrations of 3.3, 5.5, and 7.9 ppm. This effect was implemented for higher TiO_2 NPs content (0.4%) as the best catalyst efficiency (AC / CS / TiO_2 (0.4%)). Figure 6. shows the degradation efficiency of the different primary dyes. The rate of photolysis of the RB dye depends on the potential for formation of OH radicals on the surface of the catalyst and the interaction of the dye molecules with an OH-radical. The rate of photolysis decreased with increasing RB concentration. This is because as the number of RB dye molecules increases, the amount of light (the amount of photons) that penetrates the dye solution to reach the surface of the catalyst decreases due to the obstacle in the light path. Thus, the optimum value of the catalyst and the dye concentration must be maintained, so that the maximum efficiency of hydrolysis can be achieved (Gupta et al. 2012; Tang et al. 2015).

Kinetic model

The pseudo first order kinetic model was shown in figure7 by plotting Ln (a-x) against time (t). Where (a) is the initial concentration of the RB dye in (mg/l), x is the concentration at any other time t which is synonymous to the degradation rate and k is a rate constant. K is the measure of the adsorption coefficient of the reactant onto the semiconductor particles and t is the reaction time. Figure 7 shows the pseudo first order kinetic model by plotting Ln (a-x) against time (t). Where (a) is the initial RB dye concentration in milligrams per liter, x is the concentration at any other time t, which is correlated with the degradation rate, and k is a rate constant. The adsorption coefficient of the reactant onto the semiconductor particles is measured by K, and the reaction time is measured by t.The experiments were carried out using 0.1g of different catalysts with 7.9 ppm of RB dye concentration. It was found that the rate of reaction was increased when composite was used in comparison to CS/AC and TiO_2 catalysts, respectively, as indicated by the values of rate constant (k) (0.008, 0.01 and 0.02 min^{-1}) for CS/AC, TiO_2 and CS/AC/TiO_2(0.4%), respectively. The experiments have been carried out with 0.1g of various catalysts and a concentration of 7.9 ppm of RB dye. As shown by the values of rate constant (k) (0.008, 0.01, and 0.02 min^{-1}) for CS/AC, TiO_2, and CS/AC/TiO_2(0.4 %), respectively. the rate of reaction was increased when composite was used in comparison to CS/AC and TiO_2 catalysts.

Biological activities

Antibacterial activity

The antibacterial performance of a prepared CS/AC at different concentrations of TiO_2 NPs composites were evaluated by broth inhibition approach. From the data obtained in table 4 and figure 8, we can observe that, all the prepared composites with different concentration of TiO_2 NPs showed antibacterial activity against reference strains used. As well as the higher concentration of TiO_2 NPs with CS/AC brought about the higher antibacterial activity for all model bacteria used. Based on the OD and percent

of growth inhibition against the four models of bacteria, the higher antibacterial activities were observed for both B. subtilis and S. aureus followed by P. aeruginosa and then E. coli for all composites of CS/AC at different concentrations of TiO_2 NPs. We can conclude that, the prepared composites of CS/AC at different concentration of TiO_2 NPs have high antibacterial activity and an inhibit the growth of bacteria and are therefore believed to have great potential for use as antibacterial composites. Due to its chemical stability, non-toxicity, and availability, TiO2 has been demonstrated as a favorable antibacterial agent and fabricated with CS in several studies According to their chemical stability, non-toxicity, and availability of TiO_2, it was demonstrated as a favorable antibacterial agent and fabricated with CS in several studies (Raut et al. 2016; Li et al. 2019b; Moqeet Hai et al. 2019). Other studies reported the action of AC with TiO2 as antimicrobial agents (Yang et al. 2012; Ren et al. 2020).

Table 4: OD of the prepared composites against the model bacteria.

Organism	OD after 24 hs			
	Sample			
	Control	1	2	3
E. coli	2.33	2.16	1.95	1.82
P. aeruginosa	2.05	1.36	0.96	0.13
B. subtilis	2.02	0.20	0.13	0.07
S. aureus	3.04	0.71	0.35	0.11

Larvicidal and pupicidal activity.

The CS/AC/TiO_2 NPs synthesized was effective with the larvae and pupae of *C. pipiens.* The larvae's of *C. pipiens* were present highly susceptible to the synthesized CS/AC/TiO_2 than the pupae at the same concentrations of TiO_2 NPs. The mortality could be observed after 24 h of treatment. The larvae of *C. pipiens* were found highly susceptible to the synthesized CS/AC/TiO_2 (0.4%) than the same larvae at CS/AC/TiO_2 (0.2 and 0.8%). The mortality was recorded after 24 h. The soon three instars of *C. pipiens* were observed for more susceptible to the synthesized CS/AC/$TiO_2$and exhibit the highly mortality after 24 h of treatment. While the fourth larval instar and pupae were low susceptible to the synthesized CS/AC/TiO_2. The high value for larval mortality instars of *C. pipiens* mosquito was observed as 99.00±1.14, 95.00±1.43, 92.20±2.64 for CS/AC/TiO_2(0.4%) with first, second and third larval instars while high pupae mortality recorded 66.00±2.39 at the same concentration. The results showed that the lowest larvicidal activity of CS/AC/$TiO_2$0.8%. From previous results, we can conclude that, the CS/AC/TiO_2 samples have negligible larvicidal effect against *C. pipiens* when compared to their corresponding nanoparticles counterpart. The mechanism which causes the death of the larval instars and pupae could be due to the capability of the NPs to permeate out of the larval membrane. The silver nanoparticles in the intracellular space can link to sulfur containing proteins or phosphorus including component as DNA,

leading to the denaturation of some organelles and enzymes. Thereafter the decrease in membrane permeability and disturbance in proton motive force causes loss of cellular function and finally cell death Silver nanoparticles in the intracellular space can bind to sulfur-containing proteins or phosphorus-containing components such as DNA, causing organelles and enzymes to denaturate. The loss of cellular function and, eventually, cell death is caused by a decrease in membrane permeability and a disruption in the proton motive power. (J et al. 2012). At the different doses of CS/AC/TiO_2 (0.2,0.4 and 0.8%), all tested starved females of mosquito *vector C. pipiens* exhibited repellency activity. The repellent activity was varied according to their concentration, Overall, based on the recorded all doses of CS/AC/TiO_2(0.4%) was more effective in exhibiting the repellent action against *C. pipiens* starved females than another material. Similar results were also recorded by Deepalakshmi and Jeyabalan, (2017) (Deepalakshmi and Jeyabalan 2017) who tested the repellent activity of *Glochidion neilgherrense*, *Cinnamomum wightii* and *Leucas linifolia* methanol leaf extracts against *C. quinquefasciatus* and they found that all tested concentration promising mosquito repellency properties.

Table 5: Repellent activity of CS/AC/TiO_2 (0.2,0.4 and 0.8%) against mosquito vector *C. pipiens*

Material	Dose(mg/cm^2)	Unfed Females (%)	Repellency (%)
CS/AC/0.2%TiO_2	Control	6.57±1.06	0.00
	0.54	41.65±3.16	37.57±4.18
	1.31	49.67±3.06	46.02±3.91
	3.24	59.76±3.01	56.58±3.54
CS/AC/0.4%TiO_2	Control	3.9±1.99	0.00
	0.54	62.43±1.61	60.27±0.69
	1.31	70.52±3.61	68.73±3.01
	3.24	84.53±3.61	82.95±2.99
CS/AC/0.8%TiO_2	Control	4.21±2.13	0.00
	0.54	50.31±1.06	47.54±2.41
	1.31	59.01±3.64	56.97±2.61
	3.24	71.23±1.06	69.72±1.91
DEET	1.8	0.0	100.00±00

Conclusion

In this work, the fabrication of crosslinking CS / AC and CS / AC / TiO2 nanocomposite as sustainable materials for the removal of anionic dyes, such as rose bengal (RB) dye, assess its photodegradation

properties. The synthesized nanocomposites were characterized with different techniques such as SEM, FT-IR and XRD, The photo-degradation of RB shown the high efficacy of nanocomposites CS/AC/TiO_2NPs in dye as removal compared to CS/AC. The antibacterial activities of the fabricated CS/ AC/ at different concentrations of TiO2 NPs exhibit antibacterial activity against all the model bacteria used. CS/AC/0.4% TiO2 NPs showed maximum efficacy against larvicidal activity and pupicidal of mosquito vector which recorded 99.00 ± 1.14, 95.00 ± 1.43, 92.20 ± 2.64 for first, second, and third larval instars and 66.00 ± 2.39 for pupal mortality, while the repellent activity reported high protection at 82.95 ± 2.99 with 3.24 mg / cm^2 dose compared to control DEET.

Declarations

Authors Contributions

All authors contributed equally to this work. Preparation of the materials, characterizations and its applications were performed by MA, AE, RA, AS, MAA, HA, FA and AE. The manuscript was written by MA, AE, RA, AS, and all authors commented on the manuscript. All authors read and approved the final manuscript.

Ethics approval and consent to participate: Not applicable

Consent to Publish

All authors agreed with the content and that all gave explicit consent to submit.

Funding

The authors are grateful to National Research Centre, Giza, Egypt for financial support

Availability of data and materials: Available.

Competing Interests

The authors declare no conflict of interest.

Acknowledgments

The authors would like to acknowledge the supports from the National Research Centre, Giza, Egypt.

References

1. Adel AM, Ibrahim AA, El-Shafei AM, Al-Shemy MT (2019) Inclusion complex of clove oil with chitosan/β-cyclodextrin citrate/oxidized nanocellulose biocomposite for active food packaging. Food Packag Shelf Life 20:100307

2. Afzal MZ, Sun X-F, Liu J et al (2018) Enhancement of ciprofloxacin sorption on chitosan/biochar hydrogel beads. Sci Total Environ 639:560–569
3. Ali A, Noh NM, Mustafa MA (2015) Antimicrobial activity of chitosan enriched with lemongrass oil against anthracnose of bell pepper. Food Packag shelf life 3:56–61
4. Aragunde H, Biarnés X, Planas A (2018) Substrate recognition and specificity of chitin deacetylases and related family 4 carbohydrate esterases. Int J Mol Sci 19:412
5. Benelli G, Maggi F, Pavela R et al (2018) Mosquito control with green nanopesticides: towards the One Health approach? A review of non-target effects. Environ Sci Pollut Res 25:10184–10206
6. Bernard KA, Maffei JG, Jones SA et al (2001) II, Ngo KA, Nicholas DC, Young DM, Shi PY, Kulasekera VL, Eidson M, White DJ, Stone WB, Kramer LD: Comparison of WNV infection in birds and mosquitoes in New York State in 2000. Emerg Inf Dis 7:679–685
7. Bineesh KV, Kim D-K, Park D-W (2010) Synthesis and characterization of zirconium-doped mesoporous nano-crystalline TiO 2. Nanoscale 2:1222–1228
8. Cheung RCF, Ng TB, Wong JH, Chan WY (2015) Chitosan: an update on potential biomedical and pharmaceutical applications. Mar Drugs 13:5156–5186
9. Dai K, Zhang X, Fan K et al (2013) Hydrothermal synthesis of single-walled carbon nanotube–TiO2 hybrid and its photocatalytic activity. Appl Surf Sci 270:238–244
10. Danalıoğlu ST, Bayazit ŞS, Kuyumcu ÖK, Salam MA (2017) Efficient removal of antibiotics by a novel magnetic adsorbent: Magnetic activated carbon/chitosan (MACC) nanocomposite. J Mol Liq 240:589–596
11. Deepalakshmi S, Jeyabalan D (2017) Studies on Mosquitocidal and biological activity of endemic plants of Nilgiris Hills against filarial vector, Culex quinquefasciatus (Say) (Insecta: Diptera: Culicidae). Int J Adv Res Biol Sci 4:137–151. https://doi.org/10.22192/ijarbs.2017.04.03.016
12. Eivazzadeh-Keihan R, Radinekiyan F, Aliabadi HAM et al (2021) Chitosan hydrogel/silk fibroin/Mg (OH) 2 nanobiocomposite as a novel scaffold with antimicrobial activity and improved mechanical properties. Sci Rep 11:1–13
13. El-Wakil NA, Hassan EA, Abou-Zeid RE, Dufresne A (2015) Development of wheat gluten/nanocellulose/titanium dioxide nanocomposites for active food packaging. Carbohydr Polym. https://doi.org/10.1016/j.carbpol.2015.01.076
14. Elfeky AS, Salem SS, Elzaref AS et al (2020) Multifunctional cellulose nanocrystal /metal oxide hybrid, photo-degradation, antibacterial and larvicidal activities. Carbohydr Polym 230:. https://doi.org/10.1016/j.carbpol.2019.115711
15. Gupta VK, Jain R, Mittal A et al (2012) Photo-catalytic degradation of toxic dye amaranth on TiO2/UV in aqueous suspensions. Mater Sci Eng C 32:12–17
16. Hassan M, Abou-Zeid R, Hassan E et al (2017) Membranes based on cellulose nanofibers and activated carbon for removal of Escherichia coli bacteria from water. Polymers (Basel). https://doi.org/10.3390/polym9080335

17. J SS, K PR, Chandramohanakumar N, Balagopalan M (2012) Larvicidal Potential of Biologically Synthesised Silver Nanoparticles against < i > Aedes Albopictus<\i>. Res J Recent Sci 1:52–56
18. Jawad AH, Nawi MA (2012) Oxidation of crosslinked chitosan-epichlorohydrine film and its application with TiO2 for phenol removal. Carbohydr Polym 90:87–94
19. Jung K-W, Choi BH, Hwang M-J et al (2016a) Fabrication of granular activated carbons derived from spent coffee grounds by entrapment in calcium alginate beads for adsorption of acid orange 7 and methylene blue. Bioresour Technol 219:185–195
20. Jung K-W, Jeong T-U, Kang H-J, Ahn K-H (2016b) Characteristics of biochar derived from marine macroalgae and fabrication of granular biochar by entrapment in calcium-alginate beads for phosphate removal from aqueous solution. Bioresour Technol 211:108–116
21. Li B, Xia X, Guo M et al (2019a) Biological and antibacterial properties of the micro-nanostructured hydroxyapatite/chitosan coating on titanium. Sci Rep 9:1–10
22. Li H, Li X, Wang W et al (2019b) Ultraflexible and biodegradable perovskite solar cells utilizing ultrathin cellophane paper substrates and TiO2/Ag/TiO2 transparent electrodes. Sol Energy 188:158–163
23. Li S-C, Chu L-N, Gong X-Q, Diebold U (2010) Hydrogen bonding controls the dynamics of catechol adsorbed on a TiO2 (110) surface. Science 328:882–884
24. Lian Z, Zhang Y, Zhao Y (2016) Nano-TiO2 particles and high hydrostatic pressure treatment for improving functionality of polyvinyl alcohol and chitosan composite films and nano-TiO2 migration from film matrix in food simulants. Innov food Sci Emerg Technol 33:145–153
25. Lin Y, Kapadia R, Yang J et al (2015) Role of TiO2 surface passivation on improving the performance of p-InP photocathodes. J Phys Chem C 119:2308–2313
26. Luo J, Han G, Xie M et al (2015) Quaternized chitosan/montmorillonite nanocomposite resin and its adsorption behavior. Iran Polym J 24:531–539
27. Maneerat C, Hayata Y, Egashira N et al (2003) Photocatalytic reaction of TiO2 to decompose ethylene in fruit and vegetable storage. Trans ASAE 46:725
28. Moqeet Hai A, Ahmed M, Afzal A et al (2019) Characterization and antibacterial property of Kapok fibers treated with chitosan/AgCl–TiO2 colloid. J Text Inst 110:100–104
29. Murugan K, Babu R, Jeyabalan D et al (1996) Antipupational effect of neem oil and neem seed kernel extract against mosquito larvae of Anopheles stephensi (Liston). J Entomol Res 20:137–139
30. Onda K, Li B, Zhao J et al (2005) Wet electrons at the H2O/TiO2 (110) surface. Science 80-:308:1154–1158
31. Othman SH, Abd Salam NR, Zainal N et al (2014) Antimicrobial activity of TiO2 nanoparticle-coated film for potential food packaging applications. Int J Photoenergy 2014
32. Oz E, Koc S, Dusen OD et al (2013) Larvicidal activity of Cyclamen (Myrsinaceae) extracts against the larvae of West Nile virus vector Culex pipiens L.(Diptera: Culicidae). Asian Pac J Trop Med 6:449–452

33. Qian T, Su H, Tan T (2011) The bactericidal and mildew-proof activity of a TiO2–chitosan composite. J Photochem Photobiol A Chem 218:130–136
34. Raut AV, Yadav HM, Gnanamani A et al (2016) Synthesis and characterization of chitosan-TiO2: Cu nanocomposite and their enhanced antimicrobial activity with visible light. Colloids Surfaces B Biointerfaces 148:566–575
35. Ren Q, Zeng Z, Jiang Z, Li H (2020) Functionalization of renewable bamboo charcoal to improve indoor environment quality in a sustainable way. J Clean Prod 246:119028
36. Sharififard H, Rezvanpanah E, Rad SH (2018) A novel natural chitosan/activated carbon/iron bio-nanocomposite: Sonochemical synthesis, characterization, and application for cadmium removal in batch and continuous adsorption process. Bioresour Technol 270:562–569
37. Sharma S, Ameta R, Malkani RK, Ameta SC (2013) Photocatalytic degradation of rose Bengal by semiconducting zinc sulphide used as a photocatalyst. J Serbian Chem Soc 78:897–905
38. Shehata AZI (2019) Biological activity of Prunus domestica (Rosaceae) and Rhamnus cathartica (Rhamnaceae) leaves extracts against the mosquito vector, Culex pipiens L.(Diptera: Culicidae). Egypt Acad J Biol Sci F Toxicol Pest Control 11:65–73
39. Tang X, Tian M, Qu L et al (2015) Functionalization of cotton fabric with graphene oxide nanosheet and polyaniline for conductive and UV blocking properties. Synth Met 202:82–88
40. Williams KA, Green DWJ, Pascoe D, Gower DE (1986) The acute toxicity of cadmium to different larval stages of Chironomus riparius (Diptera: Chironomidae) and its ecological significance for pollution regulation. Oecologia 70:362–366
41. Xing Y, Li X, Zhang L et al (2012) Effect of TiO2 nanoparticles on the antibacterial and physical properties of polyethylene-based film. Prog Org Coatings 73:219–224
42. Xiong C, Pi L, Chen X et al (2013) Adsorption behavior of Hg2 + in aqueous solutions on a novel chelating cross-linked chitosan microsphere. Carbohydr Polym 98:1222–1228
43. Yang F-C, Wu K-H, Huang J-W et al (2012) Preparation and characterization of functional fabrics from bamboo charcoal/silver and titanium dioxide/silver composite powders and evaluation of their antibacterial efficacy. Mater Sci Eng C 32:1062–1067
44. Zhang X, Li Y, Guo M et al (2021) Antimicrobial and UV Blocking Properties of Composite Chitosan Films with Curcumin Grafted Cellulose Nanofiber. Food Hydrocoll 112:106337
45. Zhang X, Xiao G, Wang Y et al (2017) Preparation of chitosan-TiO2 composite film with efficient antimicrobial activities under visible light for food packaging applications. Carbohydr Polym 169:101–107
46. Zhao F, Repo E, Yin D, Sillanpää MET (2013) Adsorption of Cd (II) and Pb (II) by a novel EGTA-modified chitosan material: Kinetics and isotherms. J Colloid Interface Sci 409:174–182
47. Zhou JJ, Wang SY, Gunasekaran S (2009) Preparation and characterization of whey protein film incorporated with TiO2 nanoparticles. J Food Sci 74:N50–N56

Figures

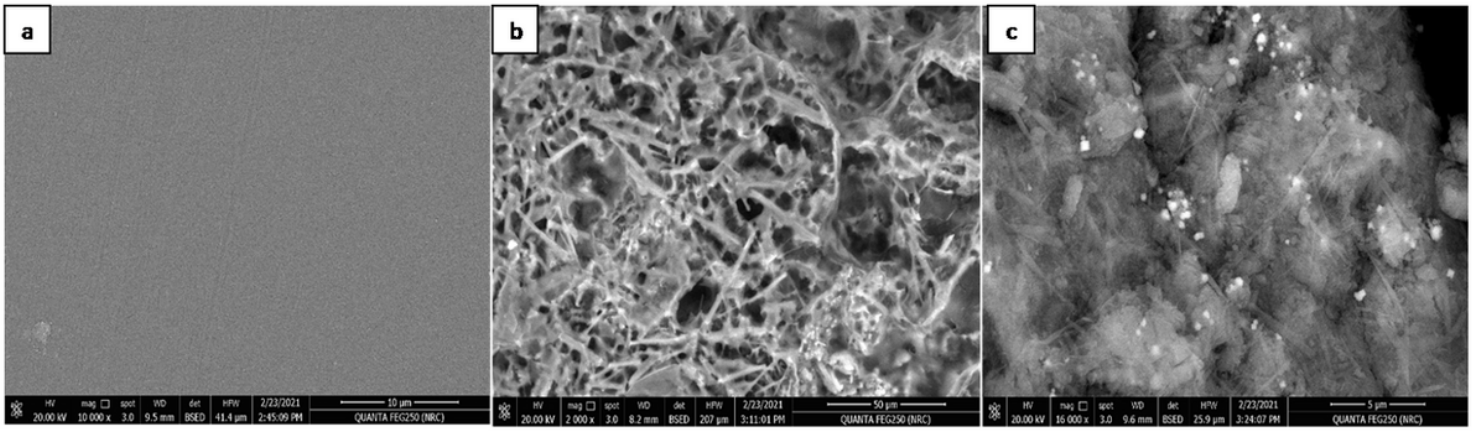

Figure 1

SEM of a) CS b) CS/AC/ECH c) CS/AC/TiO2

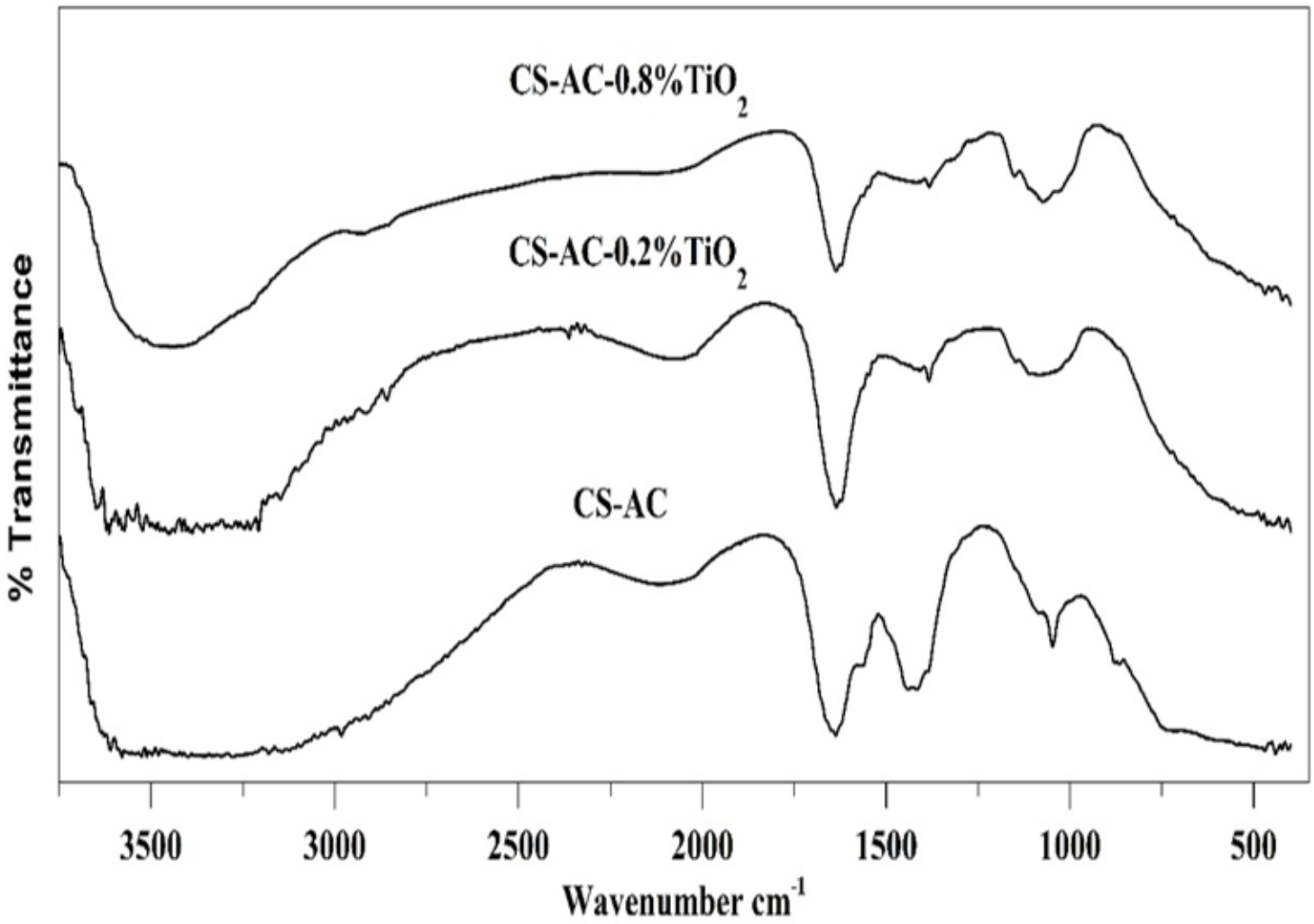

Figure 2

FT-IR spectrum of CS/AC/ECH and CS/AC/TiO2NPs

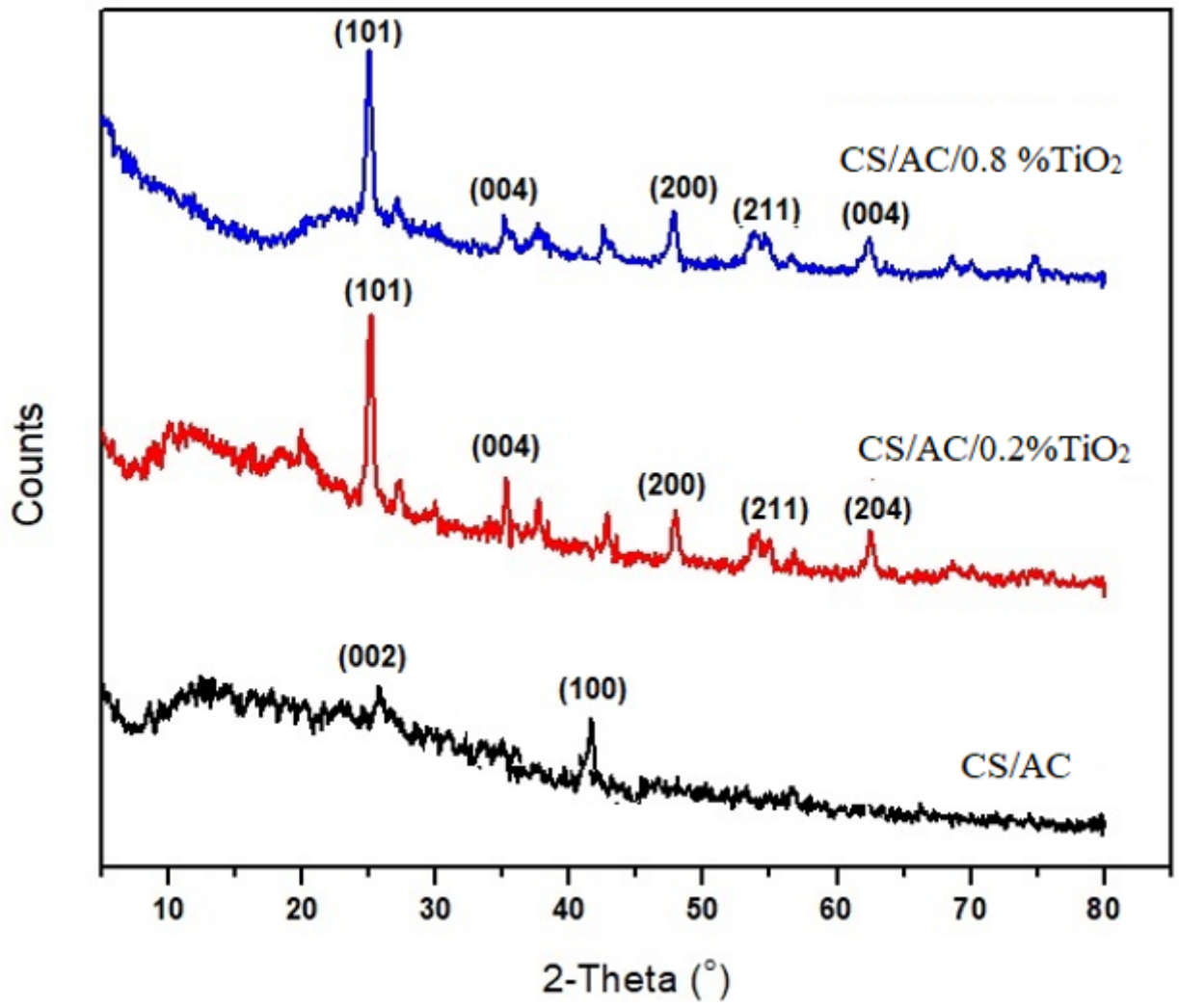

Figure 3

XRD of CS/AC/ECH and CS/AC/TiO2 NPs

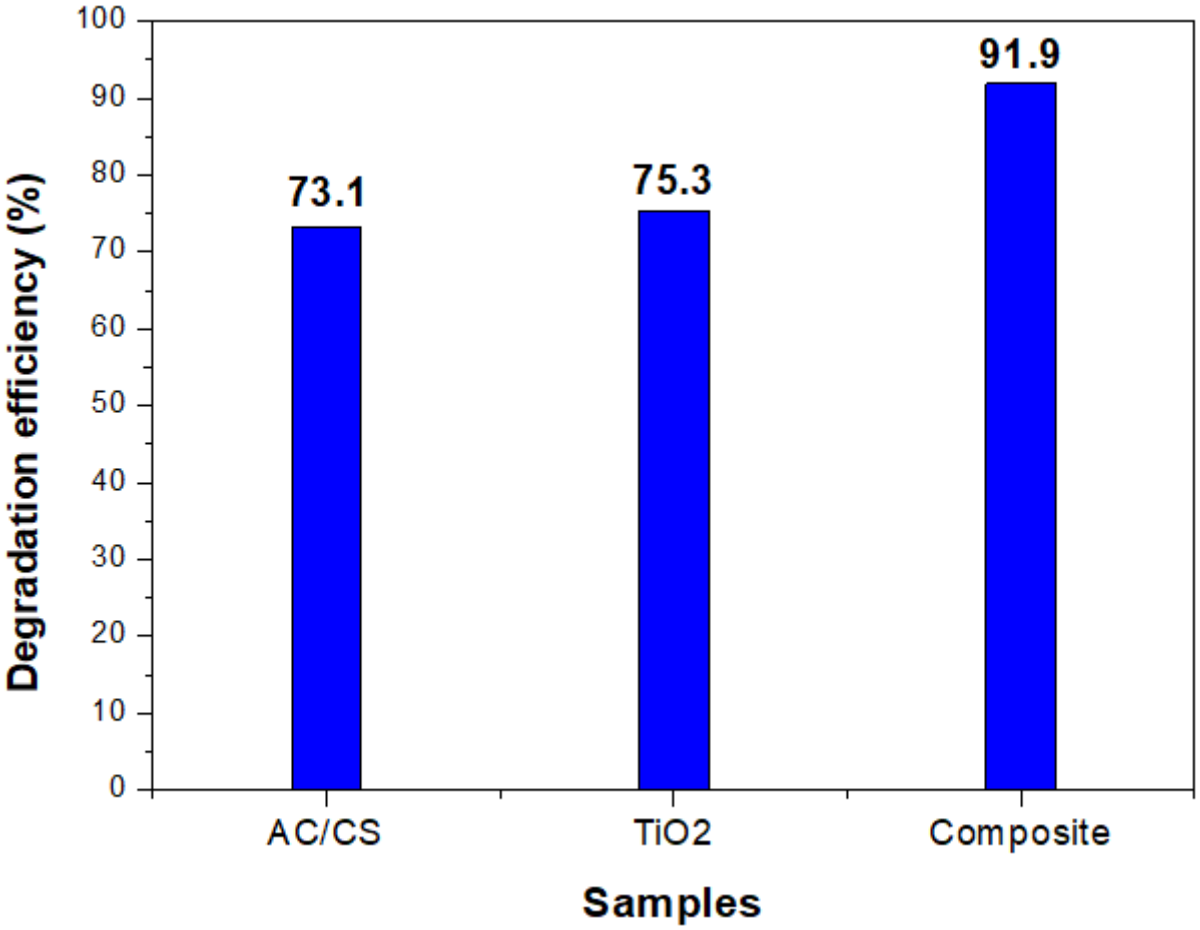

Figure 4

Photocatalytic degradation efficiency of CS/AC, TiO2 and CS/AC/TiO2.

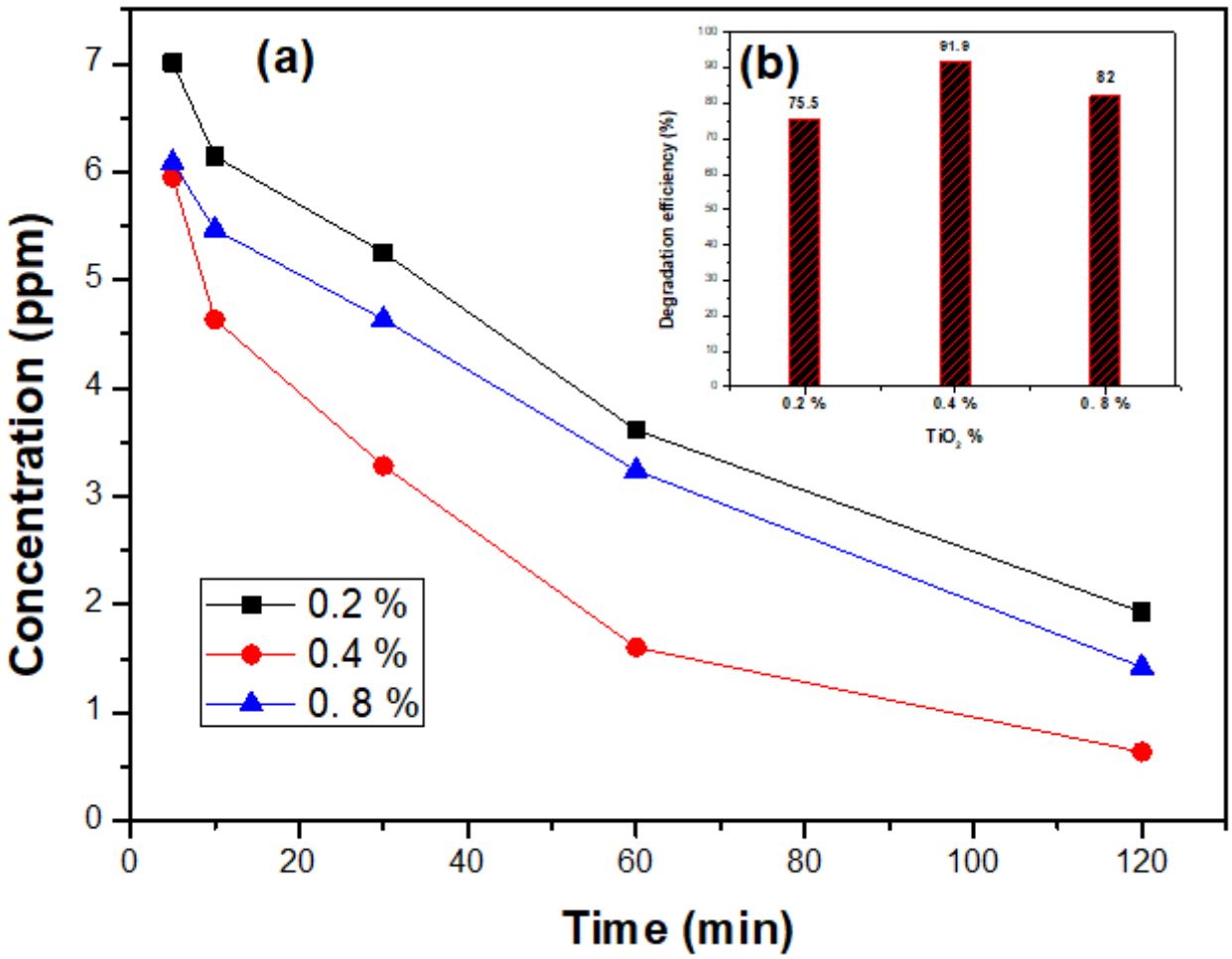

Figure 5

(a) Photodegradation of RB dye at different contents of TiO2 NPs in composite and (b) photodegradation efficiency.

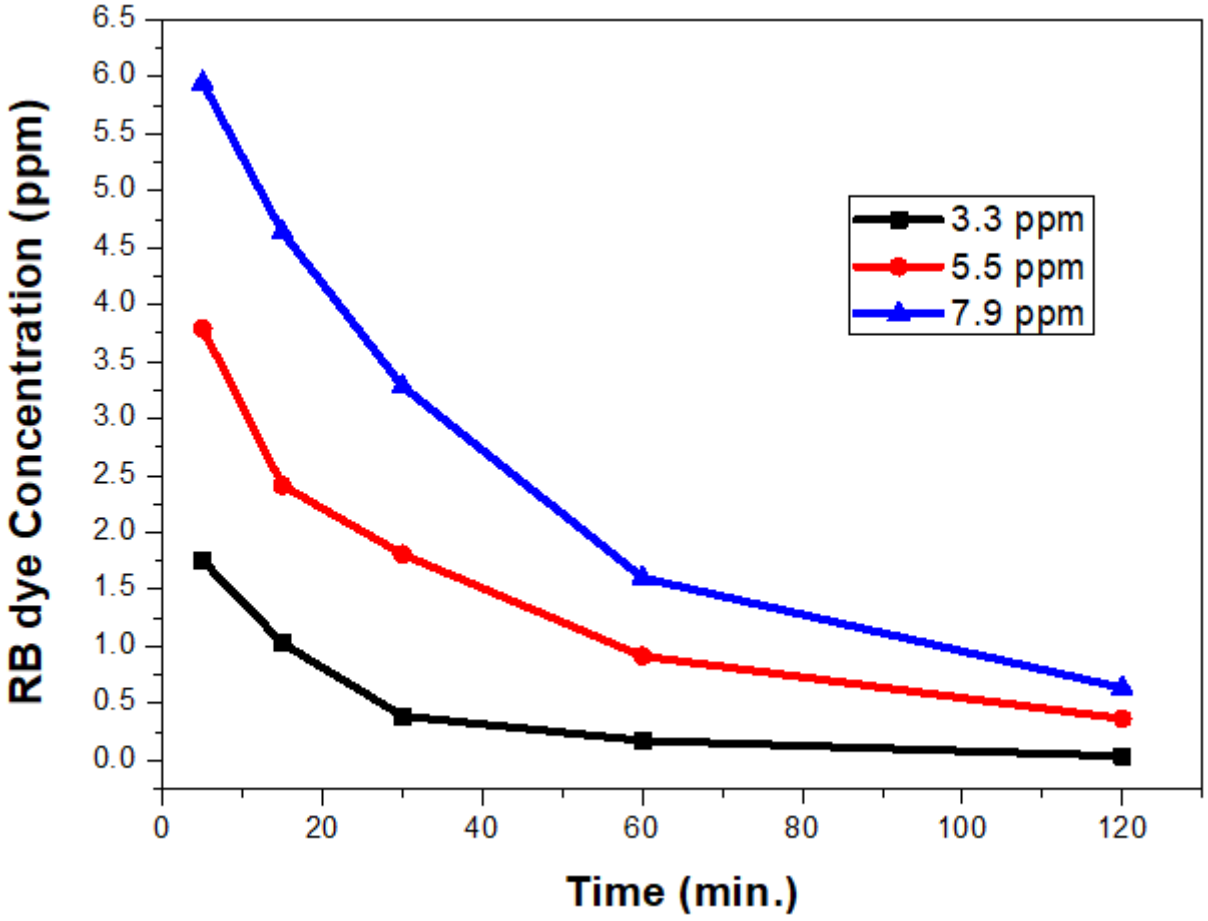

Figure 6

The effect of initial concentration of RB dye on photodegradation efficiency of composite.

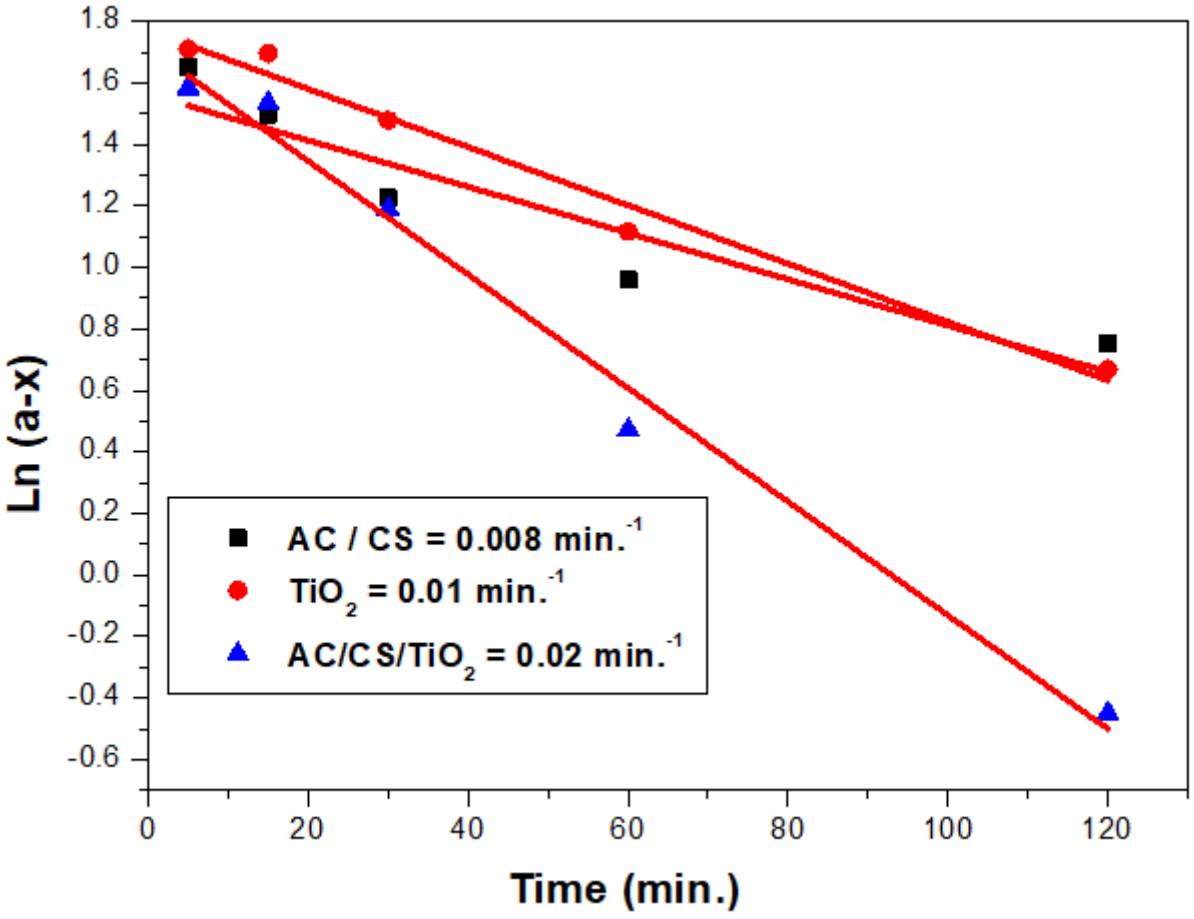

Figure 7

Kinetics of photodegradation of RB with CS/AC, TiO2 and CS/AC/TiO2.

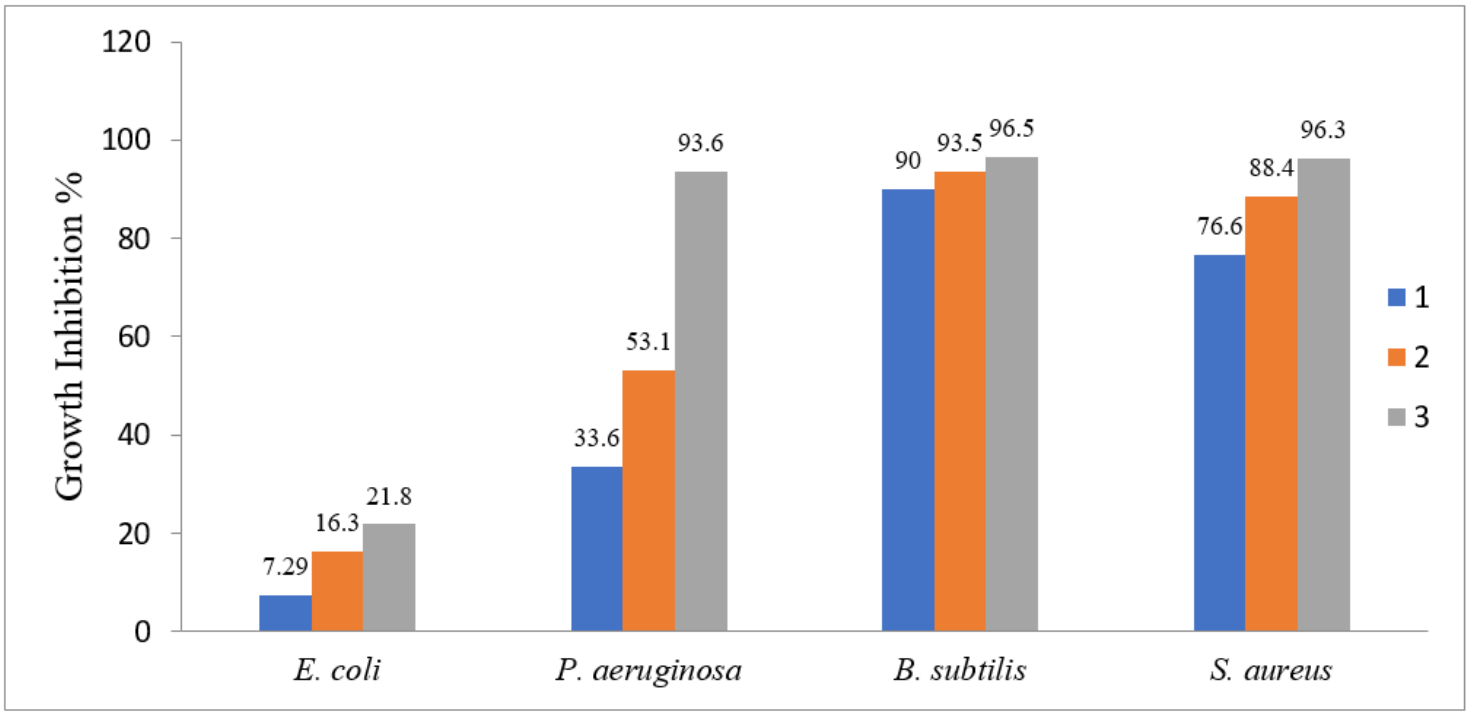

Figure 8

Growth inhibition of prepared composites against the model bacteria. Sample (1): CS/AC/0.2 TiO2NPs Sample (2): CS/AC/0.4 TiO2NPs Sample (3): CS/AC/0.8 TiO2NPs

Supplementary Files

This is a list of supplementary files associated with this preprint. Click to download.

- Scheme1.png